

Structure–Activity Relationship Studies in Single-Site Esterase Peptide Dendrimers

SACHA JAVOR AND JEAN-LOUIS REYMOND*

Department of Chemistry and Biochemistry, University of Berne, Freiestrasse 3, CH-3012, Berne, Switzerland

(Received 6 August 2008 and in revised form 4 November 2008)

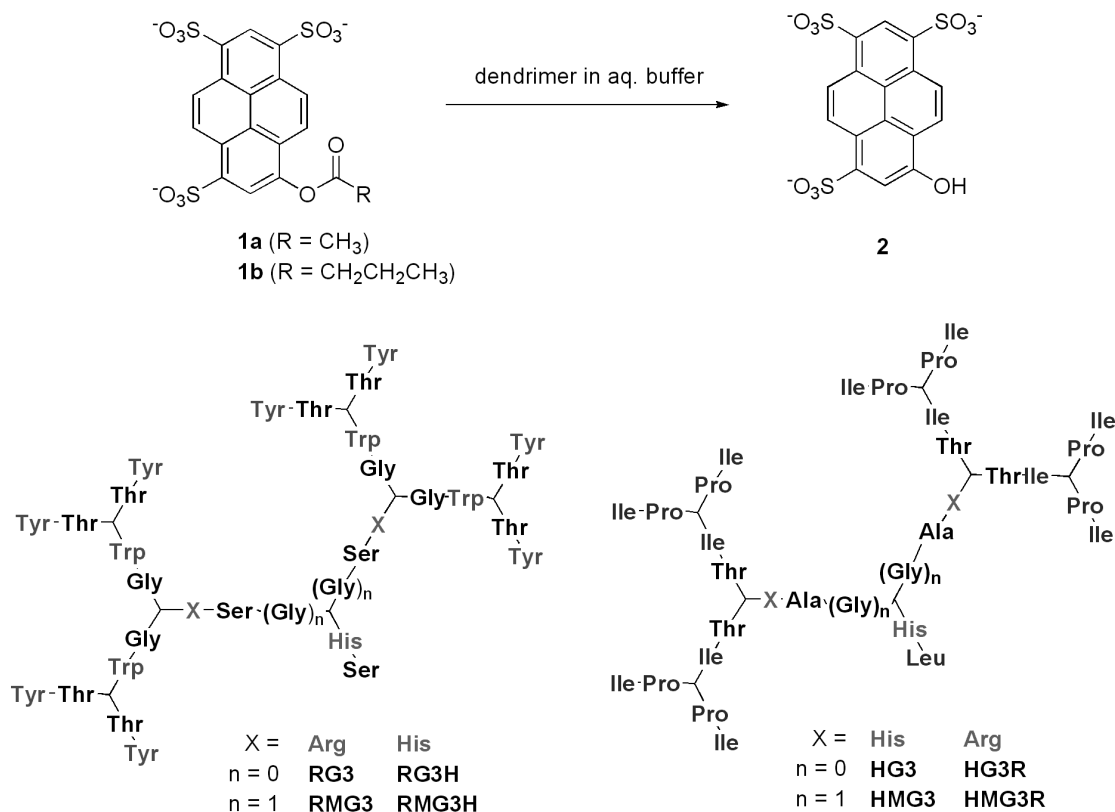
Abstract. We recently reported on peptide dendrimers with a single catalytic site at the dendrimer core catalyzing the hydrolysis of acetoxy- and butyryloxy-pyrene trisulfonate **1a/b** in aqueous buffer with Michaelis–Menten kinetics. Substrate binding is mediated by a pair of protonated arginine or histidine residues in the first generation branch, and esterolysis is performed by the imidazole side-chain of a histidine residue in the core acting as a general base or nucleophile. Herein we report on a structure–activity relationship study searching for an optimal combination between amino acid sequence and catalytic machinery. Installation of histidine residues onto the aromatic dendrimer framework “R” leads to 10-fold higher rate acceleration up to $k_{\text{cat}}/k_{\text{uncat}} = 1.5 \cdot 10^3$ at pH 5.5 with dendrimers **RG3H** (AcYT)₈(BWG)₄(BHS)₂BHS and **RMG3H** (AcYT)₈(BWG)₄(BHSG)₂BHS (one-letter codes for L-amino acids; Ac = acetyl, B = L-2,3-diaminopropionic acid branching point, C-terminus is amide –CONH₂). These dendrimers reach the compactness of a native folded protein.

INTRODUCTION

Due to their globular shape, dendrimers¹ are attractive synthetic models for proteins, in particular as catalysts.² In recent years we have shown that peptide dendrimers³ assembled by solid-phase peptide synthesis using proteinogenic amino acid building blocks and branching diamino acids may exhibit a variety of protein-like functions, such as catalysis, cofactor and protein binding, and drug delivery.^{3c} Peptide dendrimers are particularly attractive as enzyme models⁴ since they are formed from the same building blocks as natural enzymes and only differ in their topology. We have recently identified peptide dendrimers with a variety of protein-like functions by screening combinatorial libraries of dendrimers.⁵ These included peptide dendrimers with esterase-like⁶ and aldolase-like catalysis,⁷ cofactor-binding dendrimers,⁸ and multivalent glycodendrimers for lectin recognition.⁹

Peptide dendrimers can be easily modified by variations of the amino acid building blocks, which allows one to assess structure–activity relationships (SAR) that may not be accessible in other synthetic dendrimers less amenable to modifications. In the case of multivalent esterase dendrimers featuring multiple histidine residues as catalytic and binding groups,¹⁰ such SAR studies showed that histidine multivalency primarily influenced substrate binding, whereas the catalytic rate constant k_{cat} was more strongly influenced by the nature of other amino acids in the dendrimers and the exact placement of histidine residues within the structure.¹¹ Catalysis also depended on dendrimer size, with the occurrence of a positive dendritic effect on substrate binding and catalysis, as evidenced by the investigation of dendrimers at various generation numbers.

*Author to whom correspondence should be addressed.
E-mail: jean-louis.reymond@ioc.unibe.ch



Scheme 1. Esterase peptide dendrimer catalyzed hydrolysis of acyloxypyrene trisulfonates **1a/b**.

We recently reported a series of dendrimer esterase models with a single catalytic site at the dendrimer core.¹² These dendrimers catalyzed the hydrolysis of acyloxypyrene trisulfonates **1a/1b** in aqueous buffer with Michaelis–Menten kinetics. Substrate binding was mediated by a pair of protonated arginine or histidine residues in the first generation branch, and esterolysis was performed by the imidazole side-chain of a histidine residue in the dendrimer core acting as a general base or nucleophile (Scheme 1). An initial series of dendrimer analogues addressed the role in catalysis of the outer, non-catalytic layers of the dendrimers and of the relative placement of catalytic residues within the core. Herein we report further SAR studies concerning the search for an optimal combination between dendrimer sequence and catalytic machinery. We show that installation of histidine residues onto the aromatic dendrimer framework “R” leads to a 10-fold gain in rate acceleration. The combination showing enhanced activity is also the most compact as measured by hydrodynamic radius.

EXPERIMENTAL

Peptide Dendrimer Synthesis

Peptide dendrimers were synthesized by the Fmoc strategy using a Chemspeed PSW 1100 automatic synthesizer. Prior to every reaction the resin was swelled in CH₂Cl₂. The resin NovaSyn TGR was acylated with each amino acid or diamino acid (3.0 equiv) using procedures BOP (3.0 equiv) and DIEA (5.0 equiv) in a mixture of NMP/DCM (3:1) for 2 h. To ensure the completion, all the acylation steps were repeated twice. The Fmoc protecting groups were removed with a solution of 20% piperidine in DMF (2 × 20 min). At the end of the synthesis, the resin was acylated with acetic anhydride/CH₂Cl₂ (1:1) for 20 min. The cleavage was carried out with TFA/TIS/H₂O (94:5:1) for 6 h. The peptide was precipitated with methyl tert-butyl ether, and then dissolved in a water/acetonitrile mixture. All dendrimers were purified by preparative HPLC and obtained as TFA salts after lyophilization.

(((Ac-Tyr-Thr)₂Dap-Trp-Gly)₂Dap-His-Ser)₂Dap-His-Ser-NH₂ (RG3H): Starting with 250 mg of NovaSyn TGR resin (0.23 mmol/g), the dendrimer RG3H was obtained as a colorless foamy solid using the automated synthesis after cleavage

from the resin and preparative RP-HPLC purification (1.9 mg, 0.7%). MS (ES+) calcd for $C_{220}H_{278}N_{55}O_{64}$ [M+H]⁺: 4714.0. Found: 4716.8; [M+Na]⁺: 4736.0. Found: 4738.4.

((Ac-Tyr-Thr)₂Dap-Trp-Gly)₂Dap-His-Ser-Gly)₂Dap-His-Ser-NH₂ (RMG3H): Starting with 250 mg of NovaSyn TGR resin (0.23 mmol/g), the dendrimer RMG3H was obtained as a colorless foamy solid using the automated synthesis after cleavage from the resin and preparative RP-HPLC purification (1.0 mg, 0.3%). MS (ES+) calcd for $C_{224}H_{284}N_{57}O_{66}$ [M+H]⁺: 4828.1. Found: 4830.4; [M+Na]⁺: 4850.1. Found: 4852.0; [M+K]⁺: 4867.1. Found: 4871.4.

((Ac-Ile-Pro)₂Dap-Ile-Thr)₂Dap-Arg-Ala)₂Dap-His-Leu-NH₂ (HG3R): Starting with 250 mg of NovaSyn TGR resin (0.23 mmol/g), the dendrimer HG3R was obtained as a colorless foamy solid using the automated synthesis using procedure A after cleavage from the resin and preparative RP-HPLC purification (18.4 mg, 7.0%). MS (ES+) calcd for $C_{195}H_{330}N_{53}O_{49}$ [M+H]⁺: 4198.5. Found: 4200.0.

((Ac-Ile-Pro)₂Dap-Ile-Thr)₂Dap-Arg-Ala-Gly)₂Dap-His-Leu-NH₂ (HMG3R): Starting with 250 mg of NovaSyn TGR resin (0.23 mmol/g), the dendrimer HMG3R was obtained as a colorless foamy solid using the automated synthesis after cleavage from the resin and preparative RP-HPLC purification (7.1 mg, 2.7%). MS (ES+) calcd for $C_{199}H_{336}N_{55}O_{51}$ [M+H]⁺: 4312.5. Found: 4312.8

Kinetic Assays

Kinetic measurements were carried out using a CytoFluor Series 4000 multi-well plate reader from PerSeptive Biosystems. Dendrimers were used as 10 μM or 15 μM freshly prepared solutions in milliQ water. Solutions were prepared by dissolving the dry TFA salts of dendrimers. Substrate solutions for the Michaelis–Menten kinetics were prepared by serial dilution by a factor 2/3 (7×) of a freshly prepared 3.0 mM solution of substrate in milliQ water (final concentration on the plate 60–1000 μM). Low K_M determinations were carried using 30–440 μM final substrate concentrations. Eight solutions of 8-hydroxypyrene-1,3,6-trisulfonic acid sodium salt **2** ranging from 0 μM to 100 μM in buffer were used for the calibration curve. Bis-Tris 30 mM or citrate 15 mM was used as buffer and the pH was adjusted to the desired value with HCl 1.0 M and NaOH 1.0 M using a Metrohm 692 pH/ion meter. In a typical experiment, using a multichannel pipette, 40 μL of dendrimer was mixed with 40 μL of buffer and 40 μL of substrate in a Costar flat-bottom polystyrene 96-well-plate 150 μL. The formation of **2** was followed by fluorescence emission using absorbance filter 450/50 and emission filter 530/25. The gain was adjusted using the signal of the calibration curve prior to every experiment (typically a signal 45000–55000 for the 100 μM **2** well). The calibration curve (40 μL **2**, 40 μL buffer, and 40 μL H₂O) and the blank (40 μL substrate, 40 μL buffer, and 40 μL H₂O) were recorded for every experiment at the same time. The temperature inside the instrument was adjusted to 34.0 °C. Kinetic experiments typically were followed for 180 min. The data points were measured every 90 s. Fluorescence data were converted to product concentration by means of the calibration curve. Initial reaction rates were calculated from the steepest linear part observed in the curve that

gives fluorescence vs. time, typically between 500 and 2000 s, corresponding to less than 10% conversion. Michaelis–Menten parameters k_{cat} (rate constant) and K_M (Michaelis constant) were determined from the linear double reciprocal plot $1/V_{net}$ vs. $1/[S]$ (Lineweaver–Burk plot).

Diffusion-NMR

The diffusion constants of the dendrimers were obtained by ¹H NMR using a stimulated echo (STE) pulse sequence. The measurements were carried out using a Bruker DRX400 or DRX500 with dilute solutions (typically 5 mg·mL⁻¹) in D₂O at 300 K. The gradient with a maximum strength of $50 \times 10^{-4} T \cdot cm^{-1}$ was calibrated using the HOD proton signal in 99.997% D₂O. The diffusion time Δ was 50 ms and the gradient duration δ was 7 ms. The diffusion coefficient D was derived from peak integrals or intensities using the Simfit software from Bruker. The hydrodynamic radii were calculated from the diffusion coefficient D using the Stokes–Einstein equation with $\eta = 1.089$ mPa for D₂O at 300 K. The compaction factor was calculated as originally proposed.¹³

RESULTS AND DISCUSSION

In searching for core active site esterase activity in a combinatorial library of peptide dendrimers using a solid-supported assay, we had identified two types of amino acid sequences leading to activity.¹² In the first case, **RG3**, the core active site catalytic histidine was assisted by a pair of arginine residues in the 1st generation branch for substrate binding, and this core was surrounded by 2nd- and 3rd-generation layers containing the aromatic residues tryptophan and tyrosine. In the second case, **HG3**, the catalytic core displayed three histidine residues presumably sharing substrate binding and catalytic functions, and was surrounded by outer layers of aliphatic hydrophobic amino acids.

Dendrimers **RG3** and **HG3** both proved catalytically active, but they differed in the pH profile of substrate binding. The K_M value was pH-independent in the case of **RG3**, as expected from a salt-bridge interaction between the protonated arginine side chains and the sulfonate group on substrate **1a/b**. On the other hand, K_M increased with increasing pH in the case of **HG3**, reflecting the neutralization of the protonated histidines involved in a similar salt-bridge, resulting in weaker substrate binding. Both dendrimers exhibited a comparable increase in the catalytic rate constant upon increasing pH. Overall, the strong substrate binding of **RG3** at neutral pH led to an increase in catalytic proficiency of this dendrimer compared to acidic conditions, while **HG3** did not show increased activity at that pH. Most interestingly, the catalytic proficiency of **RG3** depended on the presence of the outer layer of aromatic amino acids, and was thus much more active than its lower generation analogues **RG0**→**RG2**. By contrast, **HG3** showed catalytic

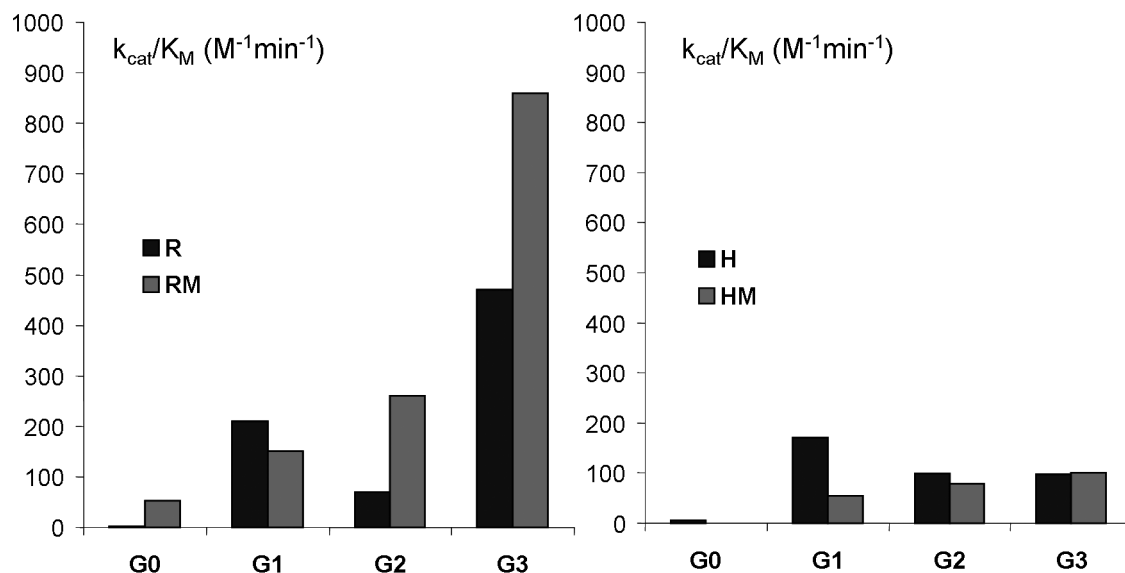


Fig. 1. Catalytic proficiencies of peptide dendrimers as a function of generation number, for the hydrolysis of substrate **1b**. Conditions: 3.3, 5.0, or 10 μM dendrimer, 30–1000 μM substrate 10 mM aq. Bis-Tris buffer pH 6.9, 34 $^{\circ}\text{C}$. Data from ref 12.

parameters that were very similar to its lower generation analogues **HG0**→**HG2**, and its outer layers of hydrophobic amino acids seemed not to play any significant role in catalysis. The kinetic parameters with the butyrate ester **1b** are representative of these trends (Fig. 1).

The existing SAR data indicated that the positive dendritic effect on catalysis was determined by the nature of the G2 and G3 layers. However, it is also conceivable that the positive effect observed in the R series on catalysis at pH 7 might depend on the presence of arginine residues for strong substrate binding. In this case one would expect to see enhanced catalysis for the **HG3** and **HMG3** dendrimers by exchanging the pair of histidine residues at G1 for a pair of arginine residues. On the other hand, combining the “R” series framework of **RG3** and **RMG3** for substrate binding with histidine residues at G1 for efficient catalysis might lead to enhanced catalytic activity if the assigned

effect of the non-catalytic aromatic amino acids was indeed correct.

To probe the contributions of the cationic residues at G1 to the positive dendritic effect, we set out to investigate the kinetic parameters of all possible exchange mutants in the form of **RG3H**, **RMG3H** for the arginine-to-histidine exchanges in **RG3** and **RMG3**, and **HG3R** and **HMG3R** for the histidine-to-arginine exchanges in **HG3** and **HMG3**, respectively. The four dendrimers were prepared by solid-phase synthesis on tentagel TGR resin as previously described using Fmoc chemistry (Table 1).

All four dendrimers were catalytically active for the hydrolysis of acyloxypyrene trisulfonates **1a** and **1b**. The kinetic parameters for the hydrolysis of these two substrates were determined in aqueous buffer at pH 5.5 and pH 6.9 (Fig. 2). The kinetic parameters of the four analogues showed remarkable differences from the parent dendrimers obtained by activity screening. As

Table 1. Synthesis of mutant single-site esterase dendrimers

no.	sequence	yield (%)	<i>m</i> (mg)	MS calcd	MS obs. ^a
RG3H	(AcYT) ₈ (BWG) ₄ (BHS) ₂ BHS	0.7	1.9	4714.0	4716.8
RMG3H	(AcYT) ₈ (BWG) ₄ (BHSG) ₂ BHS	0.3	1.0	4828.1	4830.4
HG3R	(AcIP) ₈ (BIT) ₄ (BRA) ₂ BHL	7.0	18.4	4198.5	4200.0
HMG3R	(AcIP) ₈ (BIT) ₄ (BRAG) ₂ BHL	2.7	7.1	4312.5	4312.8

^a(ES+) [M+H]⁺ peak. For the complete ion interpretation see the Supporting Information. B = branching unit (S)-2,3-diaminopropanoic acid (Dap). Amino acids indicated with one letter code. All dendrimers were pure by analytical HPLC and gave the expected signals by ¹H NMR spectroscopy.

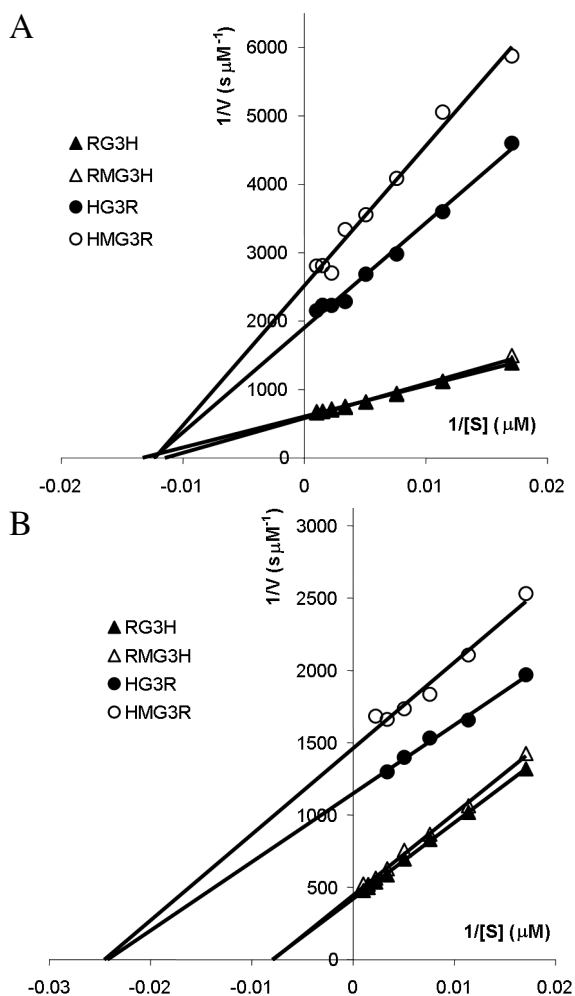


Fig. 2. Michaelis–Menten plot for dendrimers **RG3H**, **RMG3H**, **HG3R**, **HMG3R** at A: pH 5.5 and B: pH 6.9, with substrate **1b**. Conditions as in Table 2.

previously observed, the pH profile of substrate binding was primarily determined by the nature of the cationic residues at G1. Thus, the K_M values for both substrates approximately doubled between pH 5.5 and pH 6.9 for analogues **RG3H** and **RMG3H**, reflecting weaker substrate binding at higher pH due to neutralization of the positive charge in the histidines, as observed with the histidine-containing dendrimers **HG3** and **HMG3**. On the other hand the K_M values of the arginine analogues **HG3R** and **HMG3R** decreased by approximately 50% between pH 5.5 and pH 6.9, similar to the trend observed with **RG3** and **RMG3**.

The most remarkable effect in the original series concerned an increase by one order of magnitude in k_{cat} between pH 5.5 and pH 6.9 for the arginine-containing dendrimers **RG3** and **RMG3**, which was assigned to the neutralization of the core nucleophilic histidine. However, none of the analogues showed a similar effect. Thus, the k_{cat} values, at most, doubled between pH 5.5 and pH 6.9 in **HG3R/HMG3R** dendrimers, as well as in the **RG3H/RMG3H** dendrimers, which is even less than what was observed in the histidine-containing dendrimers **HG3/HMG3**. Thus, exchanging the binding residues from one dendrimer type to the other gave analogues with decreased pH-dependence of catalysis.

Analysis of the catalytic proficiency k_{cat}/K_M , which reflects the overall catalyst performance, showed that none of the analogues surpassed the original dendrimers **RG3** and **RMG3**, which have the highest catalytic proficiency in the series at pH 6.9 for the butyrate substrate **1b**. On the other hand, the introduction of histidine residues in this dendrimer type in the form of **RG3H** and **RMG3H** resulted in dendrimers retaining an excellent catalytic proficiency at pH 5.5, with values one

Table 2. Kinetic parameters for ester hydrolysis. Conditions: 3.3, 5.0, or 10 μM catalyst, 30–1000 μM substrate **1a** or **1b**, 10 mM aq. Bis-Tris buffer pH 6.9, or 5 mM citrate buffer pH 5.5, 34 °C. The formation of **2** was followed by fluorescence at $\lambda_{\text{ex}} = 450$ nm, $\lambda_{\text{em}} = 530$ nm. Under these conditions, the background rate is $k_{\text{uncat}}(\mathbf{1a}, \text{pH } 5.5) = 2.4 \times 10^{-5} \text{ min}^{-1}$, $k_{\text{uncat}}(\mathbf{1a}, \text{pH } 6.9) = 3.2 \times 10^{-4} \text{ min}^{-1}$, and $k_{\text{uncat}}(\mathbf{1b}, \text{pH } 5.5) = 1.4 \times 10^{-5} \text{ min}^{-1}$; $k_{\text{uncat}}(\mathbf{1b}, \text{pH } 6.9) = 1.3 \times 10^{-4} \text{ min}^{-1}$. The parameters are derived from Lineweaver–Burk plots with 8 data points with $r^2 > 0.95$. The error on k_{cat}/K_M is approximately ± 10 –20% based on triplicate measurements

Cpd	$100 \times k_{\text{cat}} (\text{min}^{-1})$				$k_{\text{cat}}/k_{\text{uncat}}$				$K_M (\mu\text{M})$				$k_{\text{cat}}/K_M (\text{M}^{-1} \text{min}^{-1})$			
	citrate		bis-tris		citrate		bis-tris		citrate		bis-tris		citrate		bis-tris	
	5.5	6.9	5.5	6.9	5.5	6.9	5.5	6.9	5.5	6.9	5.5	6.9	5.5	6.9	5.5	6.9
RG3	0.47	0.20	4.2	1.5	190	150	130	120	100	74	60	32	46	27	700	470
RG3H	3.7	2.1	6.1	3.1	1540	1500	190	240	103	75	199	125	360	284	305	244
RMG3	0.29	0.08	1.7	2.3	120	60	54	180	130	25	77	27	22	34	220	860
RMG3H	3.7	2.2	5.7	2.9	1540	1570	180	220	101	87	193	127	363	254	298	228
HG3	1.6	1.3	2.5	3.2	670	930	77	240	240	210	300	330	66	63	82	98
HG3R	0.68	0.68	1.5	1.1	280	490	47	85	48	81	31	41	139	84	472	272
HMG3	1.6	1.3	2.9	3.3	650	910	90	250	180	190	390	320	85	68	74	100
HMG3R	0.52	0.51	1.1	0.88	220	360	34	68	40	81	27	41	131	63	409	217

Table 3. Compaction factors C of proteins and denatured peptides and peptide dendrimers as determined by diffusion NMR. The compaction factors were calculated from the hydrodynamic radii as described in ref 14. All data are for ca. 1 mM aqueous solution (D_2O)

peptide	no. of residues	radius (nm)	C
RG3 ^a	37	1.44	0.76
RG3H	37	1.35	1.00
RMG3 ^a	39	1.52	0.65
RMG3H	39	1.34	1.09
HG3 ^a	37	1.56	0.45
HG3R	37	1.50	0.60
HMG3 ^a	39	1.62	0.40
HMG3R	39	1.54	0.58
bovine pancreatic trypsin inhibitor ^b	58	1.58	0.95
hen lysozyme ^b	129	2.05	0.93
horse cytochrome <i>c</i> (NaCl-induced molten globule) ^b	104	2.01	0.86
sperm whale apomyoglobin pH 4 (molten globule) ^b	153	2.53	0.74
residues 2–38 from D3 of fibronectin-binding protein ^{b,c}	32	1.55	0.15
hen lysozyme ^{b,c}	129	3.46	0.04

^aData from ref 12. ^bData from ref 14. ^cDetermined under strong denaturing conditions.

order of magnitude higher than those of the parent dendrimers **RG3** and **RMG3** and approximately twofold higher than the other histidine-only dendrimers **HG3** and **HMG3**.

The new dendrimer analogues **RG3H** and **RMG3H** featuring three histidine residues at the core attached to the “R” framework with aromatic amino acids in the outer layers showed the highest rate accelerations $k_{\text{cat}}/k_{\text{uncat}}$ in the series, giving values of up to $k_{\text{cat}}/k_{\text{uncat}} = 1500$ at pH 5.5, which is an order of magnitude higher than the parent “R” series dendrimers and 2–3-fold higher than the “H” series dendrimers. The effect can be traced back to the combination of efficient substrate binding as in the “R” series dendrimers with a high catalytic rate constant at pH 5.5 as in the “H” series dendrimers. The relatively modest rate accelerations $k_{\text{cat}}/k_{\text{uncat}}$ observed at pH 6.9 despite higher catalytic rate constants k_{cat} are caused by the fact that the uncatalyzed hydrolysis of the substrate in buffer (k_{uncat}) is approximately 5-fold faster at the higher pH value.

The enhanced catalytic efficiency of **RG3H** and **RMG3H** in terms of both rate acceleration $k_{\text{cat}}/k_{\text{uncat}}$ and catalytic proficiency k_{cat}/K_M at pH 5.5 is remarkable. In our initial study the higher catalytic proficiency of **RG3** and **RMG3** was correlated to their higher compaction factor, and we hypothesized that reaching a more protein-like dense packing might be beneficial for catalysis. To investigate this point, the hydrodynamic radii of the four dendrimers **RG3H**, **RMG3H**, **HG3R**, and **HMG3R** were determined by diffusion NMR, and the values were used to compute the compaction factor

(Table 3).¹³ This analysis has been used to characterize native and denatured proteins¹⁴ as well as various dendrimers.¹⁵ As in our previous study, the diffusion NMR data showed that all species were monomeric in solution. The data indicated that dendrimers **RG3H** and **RMG3H** have a significantly lower hydrodynamic radius compared to their parent dendrimers **RG3** and **RMG3**, leading to a higher compaction factor, which is of comparable value to a fully folded protein, such as bovine pancreatic inhibitor or hen lysozyme. However dendrimers **HG3R** and **HMG3R** were also more compact than the parent dendrimers **HG3** and **HMG3** despite being catalytically less active, implying that catalytic efficiency is not simply related to compactness.

CONCLUSION

The series of peptide dendrimers described above catalyzing the hydrolysis of acyloxypyrene trisulfonates in aqueous buffer using a single catalytic site at the dendrimer core were originally discovered by activity screening of a combinatorial library, which returned two possible sequence motives for catalysis. The first dendrimer type combined a core catalytic histidine residue at the core with a pair of cationic arginine residues for binding at G1 and two outer branches of aromatic amino acids at G2 at G3. The second dendrimer type displayed three histidine residues at the core and G1 for both substrate binding and catalysis, combined with outer branches of mostly hydrophobic amino acids at G2 and G3. A strong positive dendritic effect on catalytic profi-

ciency was identified in the first dendrimer type, the “R” series, and suggested that the outer layers of aromatic residues contributed positively to catalysis.

In the present study, we exchanged the catalytic machinery in these dendrimers by replacing the pair of arginine residues useful for binding with a pair of histidine residues, so as to obtain the same combination as that found in the second, “H” series dendrimers. The exchange produced two new dendrimers, **RG3H** and **RMG3H**, which display higher catalytic activity at pH 5.5, with rate accelerations up to $k_{\text{cat}}/k_{\text{uncat}} = 1500$. These new dendrimers also possess a lower hydrodynamic radius as determined by diffusion NMR and a higher compaction factor, which is similar to a folded protein. By contrast, introducing arginine residues at G1 in the “H” series dendrimers to form **HG3R** and **HMG3R** gave generally less active dendrimers compared to **HG3** and **HMG3**.

While the catalytic efficiency of our single-site esterase dendrimers for hydrolyzing acyloxypyrene trisulfonates is primarily determined by the nature of the catalytic residues in the active site, their combination with aromatic amino acids in the outer shells seems instrumental in obtaining enhanced catalytic efficiencies. Future effort will address core active site dendrimers with enhanced enzyme-like catalytic activities through efficient high-throughput screening of new libraries. The exploration of peptide dendrimers as synthetic enzyme models provides an unprecedented opportunity to explore fundamental aspects of enzyme design.

Acknowledgments. This work was supported financially by the University of Berne, the Swiss National Science Foundation, and the Marie Curie Training Network IBAAC.

REFERENCES AND NOTES

- (1) (a) Newkome, G.R.; Moorefield, C.N.; Vögtle, F. *Dendritic Molecules: Concepts, Synthesis, Applications*; VCH: Weinheim, 2001. (b) Tomalia, D.A.; Dvornic, P.R. *Nature* **1994**, *372*, 617–618. (c) Smith, D.K.; Diederich, F. *Top. Curr. Chem.* **2000**, *210*, 183–227. (d) Helms, B.; Fréchet, J.M.J. *Adv. Synth. Catal.* **2006**, *348*, 1125–1148. (e) Smith, D.K.; Diederich, F. *Chem. Eur. J.* **1998**, *4*, 1353–1361. (f) Liang, C.; Fréchet, J.M.J. *Prog. Polym. Sci.* **2005**, *30*, 385–402. Grayson, S.M.; Fréchet, J.M.J. *Chem. Rev.* **2001**, *101*, 3819–3868. (g) Lee, C.C.; Mackay, J.A.; Fréchet, J.M.J.; Szoka, F.C. *Nat. Biotechnol.* **2005**, *23*, 1517–1526.
- (2) Reviews on catalysis with dendrimers: (a) Oosterom, G.E.; Reek, J.N.; Kamer, P.C.; van Leeuwen, P.W. *Angew. Chem., Int. Ed.* **2001**, *40*, 1828–1849. (b) Twyman, L.J.; King, A.S.; Martin, I.K. *Chem. Soc. Rev.* **2002**, *31*, 69–82. (c) Kofoed, J.; Reymond, J.-L. *Curr. Opin. Chem. Biol.* **2005**, *9*, 656–664. (d) Astruc, D.; Heuze, K.; Gatard, S.; Mery, D.; Nlate, S.; Plault, L. *Adv. Synth. Catal.* **2005**, *347*, 329–338. (e) Helms, B.; Fréchet, J.M.J. *Adv. Synth. Catal.* **2006**, *348*, 1125–1148. Recent reports: (f) Wang, Z.-J.; Deng, G.-J.; Yong, L.; He, Y.-M.; Tang, W.-J.; Fan, Q.-H. *Org. Lett.* **2007**, *9*, 1243–1246. (g) Ouali, A.; Laurent, R.; Caminade, A.M.; Majoral, J.-P.; Taillefer, M. *J. Am. Chem. Soc.* **2006**, *128*, 15990–15991. (h) van de Coevering, R.; Alfers, A.P.; Meeldijk, J.D.; Martinez-Viviente, E.; Pregosin, P.S.; Klein Gebbink, R.J.M.; van Koten, G. *J. Am. Chem. Soc.* **2006**, *128*, 12700–12713. (i) Abu-Reziq, R.; Alper, H.; Wang, D.; Post, M.L. *J. Am. Chem. Soc.* **2006**, *128*, 5279–5282.
- (3) (a) Crespo, L.; Sanclimens, G.; Pons, M.; Giralt, E.; Royo, M.; Albericio, F. *Chem. Rev.* **2005**, *105*, 1663–1681. (b) Sadler, K.; Tam, J.P. *Rev. Mol. Biotechnol.* **2002**, *90*, 195–229. (c) Darbre, T.; Reymond, J.-L. *Acc. Chem. Res.* **2006**, *39*, 925–934.
- (4) (a) Kirby, A.J. *Angew. Chem., Int. Ed.* **1996**, *35*, 706–724. (b) Woggon, W.-D. *Acc. Chem. Res.* **2005**, *38*, 127–136. (c) Motherwell, W.B.; Bingham, M.J.; Six, Y. *Tetrahedron* **2001**, *57*, 4663–4686. (d) Breslow, R.; Zhang, X.; Huang, Y. *J. Am. Chem. Soc.* **1997**, *119*, 4535–4536. (e) Breslow, R.; Huang, Y.; Zhang, X.; Yang, J. *Proc. Natl. Acad. Sci. USA* **1997**, *94*, 11156–11158.
- (5) (a) Clouet, A.; Darbre, T.; Reymond, J.-L. *Angew. Chem., Int. Ed.* **2004**, *43*, 4612–4615. (b) Clouet, A.; Darbre, T.; Reymond, J.-L. *Biopolymers* **2006**, *84*, 114–123.
- (6) (a) Esposito, A.; Delort, E.; Lagnoux, D.; Djojo, F.; Reymond, J.-L. *Angew. Chem., Int. Ed.* **2003**, *42*, 1381–1383. (b) Lagnoux, D.; Delort, E.; Douat-Casassus, C.; Esposito, A.; Reymond, J.-L. *Chem. Eur. J.* **2004**, *10*, 1215–1226. (c) Douat-Casassus, C.; Darbre, T.; Reymond, J.-L. *J. Am. Chem. Soc.* **2004**, *126*, 7817–7826. (d) Clouet, A.; Darbre, T.; Reymond, J.-L. *Adv. Synth. Catal.* **2004**, *346*, 1195–1204.
- (7) Kofoed, J.; Darbre, T.; Reymond, J.-L. *Org. Biomol. Chem.* **2006**, 3268–3281.
- (8) Sommer, P.; Uhlich, N.; Reymond, J.-L.; Darbre, T. *ChemBiochem* **2008**, *9*, 689–693.
- (9) (a) Kolomiets, E.; Johansson, E.M.V.; Renaudet, O.; Darbre, T.; Reymond, J.-L. *Org. Lett.* **2007**, *9*, 1465–1468. (b) Johansson, E.M.V.; Kolomiets, E.; Rosenau, F.; Jäger, K.-E.; Darbre, T.; Reymond, J.-L. *New J. Chem.* **2007**, *31*, 1291–1299. (c) Johansson, E.M.V.; Crusz, S.A.; Kolomiets, E.; Buts, L.; Kadam, R.U.; Cacciarini, M.; Bartels, K.-M.; Diggle, S.P.; Cámara, M.; Williams, P.; Loris, R.; Nativi, C.; Rosenau, F.; Jaeger, K.-E.; Darbre, T.; Reymond, J.-L. *Chem. Biol.* **2008**, *15*, 1249–1257.
- (10) For early examples of catalytic polymers with imidazole groups: (a) Overberger, C.G.; Salamone, J.C. *Acc. Chem. Res.* **1969**, *2*, 217–224. (b) Overberger, C.G.; Mitra, S. *Pure Appl. Chem.* **1979**, *51*, 1391–1404. For other examples and reviews: (c) Suh, J. *Acc. Chem. Res.* **2003**, *36*, 562–570. (d) Benaglia, M.; Puglisi, A.; Cozzi, F. *Chem. Rev.* **2003**, *103*, 3401–3429. (e)

- Bosman, A.W.; Vestberg, R.; Heumann, A.; Fréchet, J.M.J.; Hawker, C.J. *J. Am. Chem. Soc.* **2003**, *123*, 5908–5917.
- (11) (a) Delort, E.; Darbre, T.; Reymond, J.-L. *J. Am. Chem. Soc.* **2004**, *126*, 15642–15643. (b) Delort, E.; Nguyen-Trung, N.-Q.; Darbre, T.; Reymond, J.-L. *J. Org. Chem.* **2006**, *71*, 4468–4480.
- (12) Javor, S.; Delort, E.; Darbre, T.; Reymond, J.-L. *J. Am. Chem. Soc.* **2007**, *129*, 13238–13246.
- (13) Cohen, Y.; Avram, L.; Frish, L. *Angew. Chem., Int. Ed.* **2005**, *44*, 520–554.
- (14) Wilkins, D.K.; Grimshaw, S.B.; Receveur, V.; Dobson, C.M.; Jones, J.A.; Smith, L.J. *Biochemistry* **1999**, *38*, 16424–16431.
- (15) (a) Newkome, G.R.; Young, J.K.; Baker, G.R.; Potter, R.L.; Audoly, L.; Cooper, D.; Weis, C.D.; Morris, K.; Johnson, C.S., Jr. *Macromolecules* **1993**, *26*, 2394–2396. (b) Young, J.K.; Baker, G.R.; Newkome, G.R.; Morris, K.F.; Johnson, C.S., Jr. *Macromolecules* **1994**, *27*, 3464–3471. (c) Ihre, H.; Hult, A.; Söderlind, E. *J. Am. Chem. Soc.* **1996**, *118*, 6388–6395. (d) Hecht, S.; Vladimirov, N.; Fréchet, J.M.J. *J. Am. Chem. Soc.* **2001**, *123*, 18–25. (e) Jeong, S.W.; O'Brien, D.F.; Orädd, G.; Lindblom, G. *Langmuir* **2002**, *18*, 1073–1076. (f) Fritzing, B.; Scheler, U. *Macromol. Chem. Phys.* **2005**, *206*, 1288–1291. (g) Wong, S.; Appelhans, D.; Voit, B.; Scheler, U. *Macromolecules* **2001**, *34*, 678–680. (h) Ong, W.; Grindstaff, J.; Sobransingh, D.; Toba, R.; Quintela, J.M.; Peinador, C.; Kaifer, A.E. *J. Am. Chem. Soc.* **2005**, *127*, 3353–3361.